Solar Energy Materials & Solar Cells 93 (2009) 1779–1784

Contents lists available at ScienceDirect

Solar Energy Materials & Solar Cells

journal homepage: www.elsevier.com/locate/solmat

Concentration gradient P3OT/PCBM photovoltaic devices fabricated by thermal interdiffusion of separately spin-cast organic layers

M. Kaur [a], A. Gopal [a], R.M. Davis [b], J.R. Heflin [a,*]

[a] Department of Physics, Virginia Tech, Blacksburg, VA 24061, USA
[b] Department of Chemical Engineering, Virginia Tech, Blacksburg, VA 24061, USA

ARTICLE INFO

Article history:
Received 16 December 2008
Received in revised form
13 April 2009
Accepted 7 June 2009
Available online 25 June 2009

Keywords:
Polymer solar cell
P3OT
PCBM
Interdiffusion
Auger spectroscopy

ABSTRACT

A series of organic photovoltaic devices consisting of concentration gradients of poly (3-octylthiophene) (P3OT) and [6,6]-phenyl-C_{61} butyric acid methyl ester (PCBM) were fabricated by thermally-induced interdiffusion of consecutively spin-cast layers of P3OT and PCBM from solvents of chloroform and pyridine, respectively. The device performance was evaluated as a function of the layer thicknesses, interdiffusion temperature, and interdiffusion time. A maximum power conversion efficiency of 1.0% under AM1.5G simulated solar spectrum was obtained for 70 nm P3OT thickness, 45 nm PCBM thickness, and interdiffusion at 150 °C for 20 min. Auger spectroscopy depth profiling measurements indicated that the optimal devices consist of concentration gradients of P3OT and PCBM extending across the entire film in opposite directions.

1. Introduction

Polymeric photovoltaic devices offer the potential for inexpensive, large area, lightweight, flexible efficient renewable power sources [1,2]. The highest efficiencies achieved so far are ~5% under AM1.5 simulated solar spectrum for devices made from blends of poly (3-hexylthiophene) (P3HT) and [6,6]-phenyl-C_{61} butyric acid methyl ester (PCBM) [3]. Significant efforts are being made to increase efficiencies through low bandgap polymers, new acceptor materials, and novel processing approaches, and important practical considerations such as stability and fabrication of large area devices are gaining more attention [2,4–7]. Polymeric photovoltaic devices rely upon the dissociation of a photogenerated exciton by the transfer of an electron from the P3HT donor to the PCBM acceptor species. Because the exciton diffusion distance is limited to <10 nm [8–10], it is essential to control the composition of the electron donor and acceptor components on the nanometer length scale. In standard blend (bulk heterojunction) devices, one relies on phase separation of the two components to accomplish this in an averaged manner throughout the film. Blend devices, in which the semiconducting polymer donor and fullerene acceptor are co-dissolved in an organic solvent and spin-cast into a single film, provide good charge transfer from electron donor to acceptor, but charge transport is potentially limited due to discontinuous pathways of the donor and acceptor materials to their respective electrodes. In contrast, bilayer devices provide optimized charge transport while the charge transfer is severely compromised. We have been developing an approach wherein a concentration gradient of the two components is achieved to maximize the concentration of the majority carrier component in the vicinity of each respective electrode while still providing proximity of the donors and acceptors to enable charge transfer [11–13]. This has been accomplished through sublimation of a C_{60} layer on top of a spin-cast polymer layer followed by thermally-induced interdiffusion of the two films. Here, we report on a series of experiments performed to study organic photovoltaic devices consisting of concentration gradients of poly (3-octylthiophene) (P3OT) and PCBM fabricated in a novel manner. The devices were fabricated by thermally-induced interdiffusion of consecutively spin-cast layers of P3OT and PCBM from solvents of chloroform and pyridine, respectively.

Other approaches have also been explored to obtain more complex arrangements than phase-separated blends of the donor and acceptor species. Granstrom et al. [14] separately spin-cast donor and acceptor polymers on two separate electrodes and laminated the two together at 200 °C in order to obtain partial mixing of the two layers. Chen et al. [15] spin-cast PCBM from xylene onto a film of poly[2-methoxy-5-(3′,7′-dimethyloctyloxy)-1,4phenylenevinylene] (MDMO-PPV). Since MDMO-PPV is only weakly soluble in xylene at room temperature, it was presumed that the PCBM should penetrate into the MDMO-PPV during the

* Corresponding author. Tel.: +1 540 231 4504.
E-mail address: rheflin@vt.edu (J.R. Heflin).

0927-0248/$ - see front matter © 2009 Elsevier B.V. All rights reserved.
doi:10.1016/j.solmat.2009.06.009

spin-coating process. Xue et al. sandwiched a mixture of copper phthalocyanine (CuPc) donor and C_{60} acceptor between two pure layers of CuPc and C_{60} [16].

PCBM is generally a preferred acceptor material to C_{60} for organic photovoltaic devices because the presence of the side chain enhances the solubility and the higher lowest unoccupied molecular orbital (LUMO) energy level relative to C_{60} leads to a higher open circuit voltage, V_{oc}. However, PCBM does not survive sublimation without substantial decomposition. Thus, in order to develop concentration gradient devices consisting of P3OT and PCBM for the present work, it was necessary to develop a modified fabrication procedure in which the materials are sequentially spin-cast. Furthermore, the layer thicknesses and interdiffusion temperature and time were varied in order to optimize the efficiency of the devices. It has been found with optimized parameters that P3OT–PCBM interdiffused devices can achieve a monochromatic power efficiency of ~2% at 470 nm and AM1.5G simulated solar spectrum efficiency of 1.0%. The devices were studied at different interdiffusion temperatures, with a primary focus on 140 and 150 °C. P3OT is a semicrystalline polymer with a melting point (T_m) of 187 °C and a glass transition temperature (T_g) of the order of ~100 °C [13]. Hence, annealing and interdiffusion both were carried out at temperatures above T_g but below T_m.

2. Experimental details

Indium tin oxide (ITO)-coated glass slides were spin-coated with poly (3,4-ethylenedioxythiophene):poly(styrenesulfonate) (PEDOT:PSS) complex (Bayer Corporation) at 1400 rpm. P3OT (Rieke Metals, Inc.) was spin-coated from 0.8 wt/vol% solution in chloroform at 2750 rpm followed, in some cases, by annealing of the device at 120 °C for 10 min. Annealing was done under vacuum (4×10^{-6} Torr) to remove residual water and solvents and to increase the P3OT crystallinity for improved hole mobility [3]. PCBM was then spin-cast from a 2.0 wt/vol% solution in pyridine at 2450 rpm. The P3OT thickness was varied by changing the spin speed in the range 2000–2750 rpm, while the concentration was maintained at 0.8 wt/vol%. It was found that the PCBM thickness is quite independent of the spin speed and is instead highly dependent on the amount of solution dropped onto the substrate. The PCBM thickness was thus controlled by varying the number of drops from 6 to 15 while the substrate spun at 2450 rpm. Pyridine was used as a wetting layer between P3OT and PCBM. About 10–15 drops of pyridine were applied to the substrate while it was spinning at 2450 rpm followed by PCBM immediately, without letting the pyridine dry. Interdiffusion of the devices was carried out in the vacuum chamber at different temperatures for varied intervals of time. Aluminum cathodes were then thermally evaporated onto the film after interdiffusion was completed.

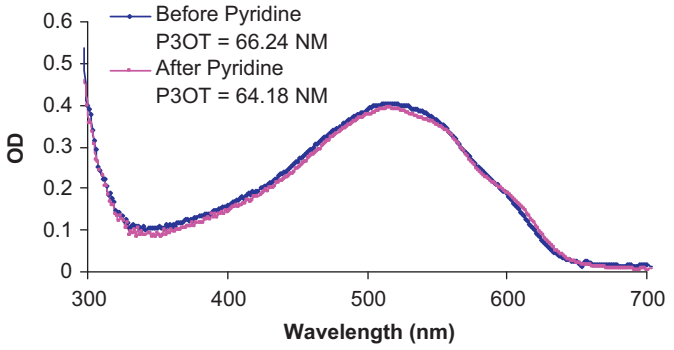

Fig. 1. Optical density of a P3OT film on glass before and after washing with 7–8 drops of pyridine while spinning at 2000 rpm.

The thickness of P3OT and PCBM films was determined from the optical density obtained from reflection and transmission measurements with a Filmetrics F20-UV thin film spectrometer system. The absorption coefficient used for P3OT is $14 \times 10^4\,cm^{-1}$ at 512 nm and for PCBM it is $2 \times 10^4\,cm^{-1}$ at 512 nm. Photocurrent spectra were measured using a 300-W Xe lamp in combination with a CVI CM 100 monochromator as the illumination source and a Keithley 485 picoammeter to record the short circuit currents I_{SC}. The power spectrum $P(\lambda)$ of the lamp was determined with a calibrated Si diode. Photoresponsivity (PR) is the conversion efficiency of light to electrical energy and is given by

$$PR(\lambda) = \frac{I_{SC}(\lambda)}{P(\lambda)} \quad (1)$$

Here $I_{SC}(\lambda)$ is the short circuit current when there is no voltage on the device and $P(\lambda)$ is the power of illumination for a specific wavelength.

EQE is the conversion efficiency of incident photons to the extracted electrons and can be determined from photoresponsivity by

$$EQE(\lambda) = \frac{hc}{e}\frac{PR(\lambda)}{\lambda}, \quad (2)$$

where h is the Planck's constant, c the speed of light, and e the charge of the electron. I–V curves were measured with a Keithley 236 source measure unit in the dark, using the 470-nm monochromatic light of the Xe lamp and using the AM1.5G simulated solar spectrum described below.

In addition to measurements under monochromatic illumination, measurements were also taken under simulated AM1.5G solar spectrum. AM0 and AM1.5G filters (Oriel Instruments), calibrated for the 300 W Xenon arc lamp, were placed in front of the lamp to produce the simulated solar spectrum. The AM1.5G solar spectrum was set to an intensity of $100\,mW/cm^2$ (1 sun) using a calibrated silicon photodiode and the results were uncorrected for spectral mismatch.

To study the concentrations of P3OT and PCBM in the interdiffused films, a 610 Perkin–Elmer scanning Auger spectroscopy system in combination with Ar-ion-beam milling was used. In this system, the surface layer of a film can be tested for its atomic constituents. After the Auger scan, the surface layer is milled off with an Ar-ion beam, and the new surface layer can be tested.

The spin-coating of a PCBM layer on a previously spin-cast layer of P3OT is critical to this work. In contrast to C_{60}, which is not very soluble but is easily sublimed, PCBM is quite soluble in a number of organic solvents but is highly susceptible to decomposition during sublimation. In order to avoid dissolution of the P3OT layer during spin-coating of PCBM, it was necessary to find a solvent in which PCBM is well-soluble but which is a poor solvent for P3OT. A variety of solvents were tested to see which can

Table 1
Monochromatic power conversion efficiency, fill factor, open circuit voltage, and short circuit current density for P3OT–PCBM bilayer devices.

Thickness	Efficiency 470 nm (%)	FF 470 nm	V_{oc} 470 nm (V)	J_{sc} 470 nm (mA/cm^2)
P3OT(85 nm) PCBM(62 nm)	0.16	0.43	0.255	−0.05
P3OT(64 nm) PCBM(45 nm)	0.23	0.42	0.345	−0.06

dissolve PCBM well compared to P3OT. It was found that pyridine dissolves PCBM fairly well but does not wash off a layer of P3OT spin-cast from chloroform. To test this, 7–8 drops of pure pyridine were dropped onto a substrate having a P3OT layer and spinning at 2000 rpm. Optical density measurements were made on the P3OT layer before and after the pyridine wash as shown in Fig. 1. It is evident from the figure that the thickness is essentially the same before and after pyridine washing. On the other hand, pyridine can dissolve PCBM at better than 25 mg/ml.

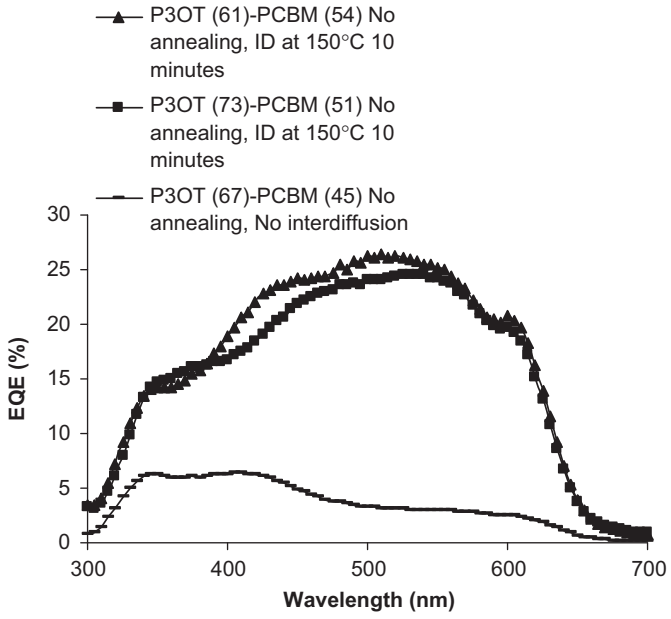

Fig. 2. EQE spectra for P3OT–PCBM devices with and without interdiffusion. Interdiffusion is carried out at 150 °C for 10 min without prior annealing. Individual film thicknesses prior to interdiffusion are indicated in parentheses.

3. Results and discussion

Initially, several P3OT–PCBM devices were made without interdiffusion, which we refer to as bilayer devices. P3OT was annealed at 120 °C prior to the PCBM deposition followed by the aluminum deposition. The bilayer P3OT–PCBM devices were found to have a monochromatic (470 nm) power conversion efficiency of ~0.2%. The 470 nm monochromatic power conversion efficiencies, fill factors (FF), open circuit voltages (V_{oc}), and short circuit current densities (J_{sc}) values are shown in Table 1.

Next, in order to determine whether the increased polymer crystallinity caused by annealing would hinder diffusion of PCBM into the polymer film, devices were fabricated both with and without annealing of the P3OT film prior to the interdiffusion step. First, several interdiffused devices were made without annealing of the P3OT layer prior to deposition of PCBM and interdiffusion. Fig. 2 shows the EQE spectra of P3OT–PCBM devices with and without interdiffusion and without prior annealing. Here interdiffusion is carried out at 150 °C for 10 min. The interdiffused devices consisted of P3OT/PCBM thicknesses of 61/54 nm and 73/51 nm. These devices had the highest efficiencies of ten devices of varying thicknesses made without P3OT annealing prior to interdiffusion. The 470 nm monochromatic and AM1.5G power conversion efficiencies, fill factors, open circuit voltages (V_{oc}), and short circuit current densities (J_{sc}) are shown in Table 2. The highest AM1.5G power conversion efficiency obtained was 0.38%. It can be seen by comparison with Table 1 that interdiffusion results in an order of magnitude increase in the monochromatic power conversion efficiencies.

For additional devices, the P3OT layer was annealed at 120 °C for 10 min prior to spin-casting of PCBM and interdiffusion. As will

Table 2
Monochromatic and AM1.5G power conversion efficiency, fill factor, open circuit voltage, and short circuit current density for interdiffusion done at 150 °C for 10 min without prior annealing.

Thickness	Efficiency 470 nm (%)	Efficiency AM1.5G (%)	FF 470 nm	FF AM1.5G	V_{oc} 470 nm (V)	V_{oc} AM1.5G (V)	J_{sc} 470 nm (mA/cm^2)	J_{sc} AM1.5G (mA/cm^2)
P3OT (61 nm) PCBM (54 nm)	1.45	0.28	0.44	0.33	0.385	0.395	−0.34	−2.65
P3OT (73 nm) PCBM (51 nm)	1.5	0.38	0.47	0.32	0.385	0.485	−0.32	−3.7

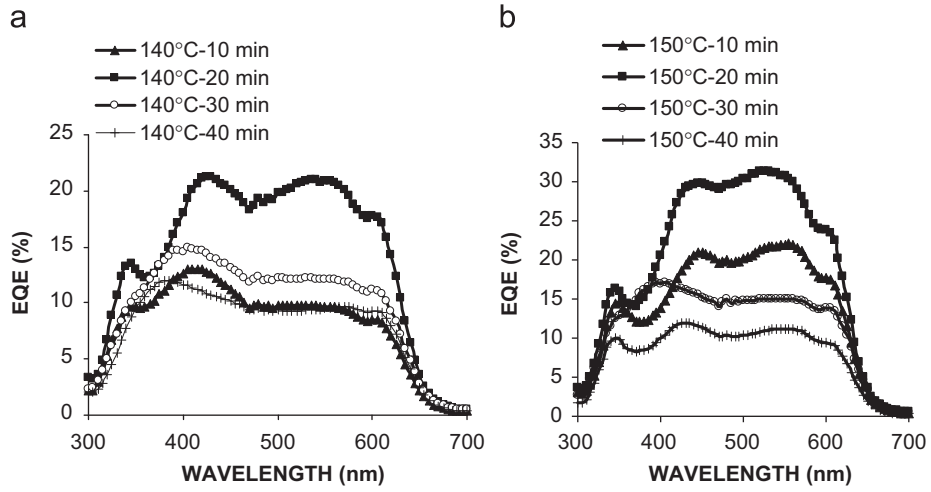

Fig. 3. EQE spectra for P3OT (70 nm)–PCBM (40–50 nm) devices interdiffused at (a) 140 °C for 10, 20, 30, and 40 min and (b) 150 °C for 10, 20, 30, and 40 min. The P3OT film was annealed at 120 °C for 10 min prior to PCBM deposition in all devices.

be seen below, the device performance was comparable to or better than devices without prior annealing. We thus concluded that the increased P3OT crystallinity induced by annealing does not interfere with the interdiffusion process and thus concentrated our efforts on devices for which the P3OT layer was annealed at 120 °C for 10 min prior to PCBM deposition.

The interdiffusion temperature and time are two major factors that affect P3OT–PCBM devices by determining the extent of interdiffusion of the two layers. Interdiffusion was done at 140 and 150 °C for varied amounts of time for devices with constant thickness of 70 nm for P3OT and 40–50 nm for PCBM. The EQE spectra for these devices are shown in Fig. 3. For interdiffusion done at both 140 and 150 °C, as the time of interdiffusion is increased from 10 to 40 min with a step of 10 min, the device with interdiffusion done for 20 min shows the highest EQE.

Fig. 4 shows the trend of the monochromatic power conversion efficiency (470 nm, 4.2 mW/cm^2) as the interdiffusion time is varied at 140 and 150 °C. Each data point is an average over 2–3 devices with the same thickness. As is evident from the figure, the maximum efficiency occurs when the interdiffusion is done for 20 min, and there is a decrease in device performance for longer interdiffusion times.

Table 3 shows the power conversion efficiency, fill factor, open circuit voltage, and short circuit current density of the P3OT–PCBM interdiffused devices under monochromatic (470 nm) as well as AM1.5 illumination. The interdiffusion is done at 150 °C for varied periods of time and the thicknesses of the P3OT and PCBM were maintained at 70 and 40–50 nm, respectively. The short circuit current density is maximized for 20 min of interdiffusion, while the open circuit voltage values are similar for 20 and 30 min of interdiffusion and the fill factor exhibits relatively modest variation.

While there are a large number of studies reported on blend bulk heterojunction devices of P3HT and PCBM, there are very few reports on P3OT/PCBM devices. One study reports a V_{oc} of 0.635 V and AM1.5G power conversion efficiency of 1.1% for 1:3 concentrations of P3OT and PCBM [17]. Another publication reports a V_{oc} of 0.60 V under 20 mW/cm^2 monochromatic illumination at 488 nm, but no results were given for simulated solar spectrum [18].

Fig. 5 compares the *J–V* curves under AM1.5G illumination for the two devices in which the P3OT layer was not annealed and devices where the P3OT layer was annealed at 120 °C for 10 min prior to PCBM deposition with interdiffusion at 150 °C for 10, 20, and 30 min. It is evident from Fig. 5 that prior annealing does not interfere with the interdiffusion of P3OT and PCBM. Furthermore, V_{oc} of the annealed interdiffused devices is higher than that of the non-annealed interdiffused devices by 0.1–0.2 V. The series resistance [19] of the annealed devices with interdiffusion at 150 °C was calculated from the slope of the *J–V* curve at high applied voltage. The series resistance is calculated using the formula

$$R_s = \left(\frac{dV}{dI}\right)_{V\to\infty} \quad (3)$$

In practice, R_s was calculated in the voltage range of 1.0–1.5 V. Series resistances of 6.63, 4.84, 3.21, and 4.1 Ω cm^2 were obtained for interdiffusion for 10, 20, 30, and 40 min, respectively, demonstrating that the series resistance generally decreases with increased interdiffusion of P3OT and PCBM. The increase in the series resistance for interdiffusion at 40 min compared to 30 min may be due to an inversion of the P3OT and PCBM to opposite electrodes that appears to occur when the interdiffusion is carried out for longer times. This is discussed further with respect to Fig. 7.

Fig. 6 shows the monochromatic power conversion efficiency with respect to the time of interdiffusion when the interdiffusion

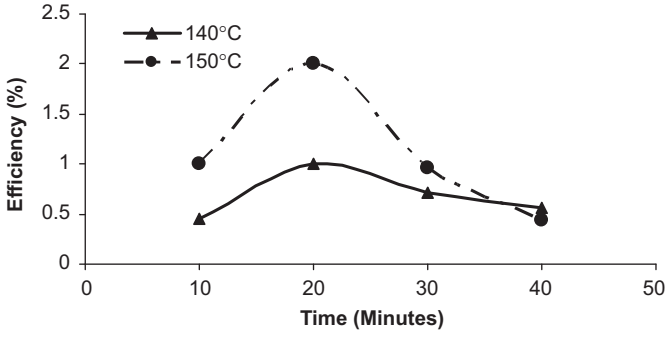

Fig. 4. Average monochromatic power conversion efficiency (470 nm, 4.2 mW/cm^2) vs. time of interdiffusion at 140 and 150 °C for devices with P3OT and PCBM thicknesses of 70 nm and 40–50 nm, respectively.

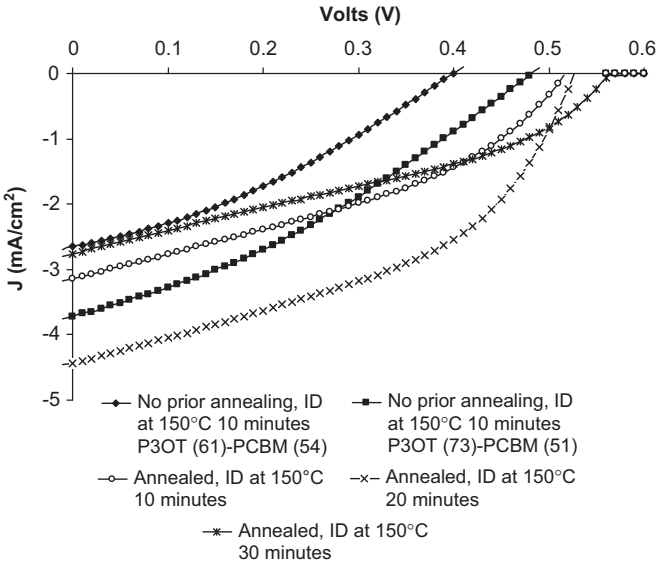

Fig. 5. AM1.5G illumination 4th quadrant *J–V* characteristics for P3OT–PCBM devices interdiffused at 150 °C for 10, 20, and 30 min.

Table 3
Monochromatic and AM1.5 power conversion efficiency, fill factor, open circuit voltage, and short circuit current density for interdiffusion done at 150 °C for varying time interval.

Interdiffusion time (min)	Efficiency 470 nm (%)	Efficiency AM1.5G (%)	FF 470 nm	FF AM1.5G	V_{oc} 470 nm (V)	V_{oc} AM1.5G (V)	J_{sc} 470 nm (mA/cm^2)	J_{sc} AM1.5G (mA/cm^2)
10	1.0	0.6	0.41	0.38	0.355	0.515	−0.272	−3.2
20	2.0	1.0	0.5	0.44	0.385	0.525	−0.395	−4.1
30	1.0	0.55	0.39	0.36	0.395	0.565	−0.247	−2.76
40	0.44	0.3	0.42	0.43	0.285	0.435	−0.141	−1.67

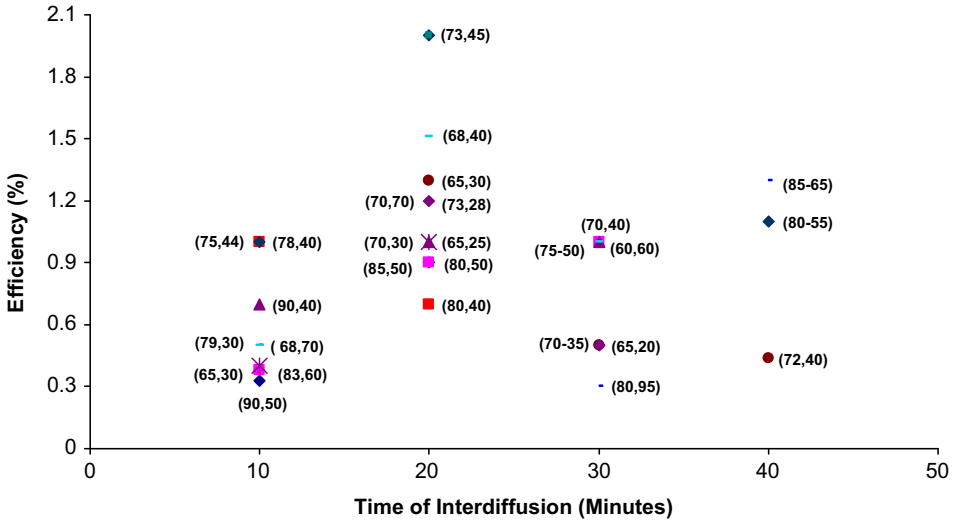

Fig. 6. Monochromatic (470 nm) power conversion efficiency vs. time of interdiffusion for varied device (P3OT, PCBM) thickness for interdiffusion at 150 °C and with annealing at 120 °C for 10 min.

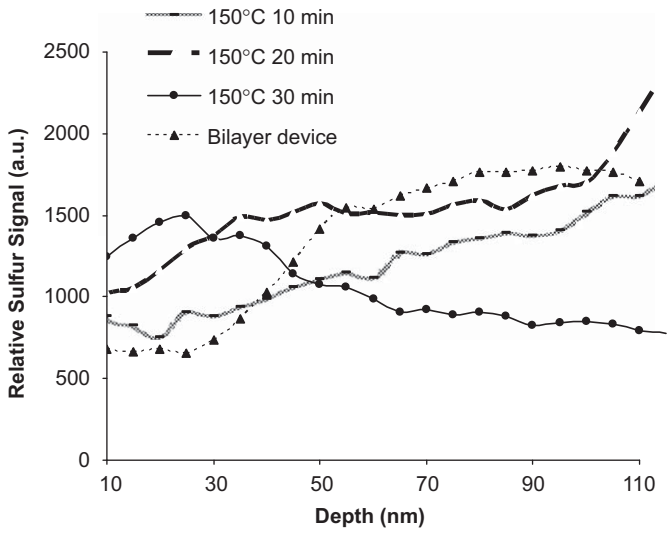

Fig. 7. Auger spectroscopy depth profiles for P3OT–PCBM bilayer and interdiffused devices with interdiffusion carried out at 150 °C for 10, 20, and 30 min.

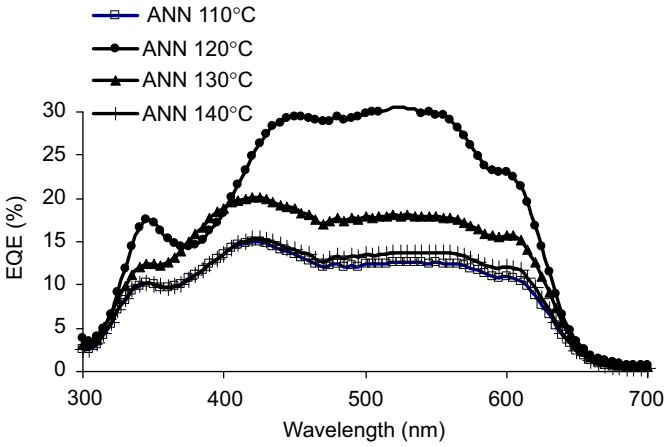

Fig. 8. EQE spectra for annealing for 10 min at temperatures of 110, 120, 130, and 140 °C with the interdiffusion carried out at 150 °C for 20 min. The thicknesses were maintained constant at 70 nm for P3OT and 40–50 nm for PCBM.

temperature is maintained at 150 °C but the thickness is varied. As it is evident from the figure, devices with a thickness of the order of 70 nm of P3OT and 40–50 nm PCBM have better efficiency. In addition, the efficiency is optimized when interdiffusion is done at 150 °C for 20 min.

Concentration depth profiles of the P3OT–PCBM films were studied using Auger spectroscopy and ion beam milling. Since P3OT contains sulfur while PCBM does not, the sulfur signal indicates the relative amount of P3OT in the film as a function of depth. The absolute intensity of the sulfur signals vary from measurement to measurement depending on the settings and sensitivity of the apparatus. Hence, the intensity of the signals is meaningful only within each scan and the magnitudes of different scans are arbitrary. Fig. 7 shows the Auger spectroscopy depth profiles for a device that was not thermally interdiffused and devices interdiffused at 150 °C for 10, 20, and 30 min. The device that was not thermally interdiffused indicates a fairly pure PCBM layer followed by a fairly pure P3OT layer with a gradient over roughly 20 nm in between. For the devices with interdiffusion done for 10 and 20 min, there is a gradually increasing concentration of P3OT from the top to the bottom of the film. For the device interdiffused for 30 min, the concentration gradient appears to reverse such that the concentration of P3OT is higher at the top of the film. While this latter result suggests that the surface energy is minimized when the polymer is at the surface, we are not aware of any published results that allow comparison of the surface energies of P3OT and PCBM.

In all the devices discussed so far, when annealing was performed the P3OT was annealed at 120 °C for 10 min prior to the spin-coating of the PCBM layer. In order to examine the effect of the annealing temperature, annealing was carried out at 110, 120, 130, and 140 °C for devices with P3OT thickness of 70 nm and PCBM thickness of 40–50 nm. The interdiffusion step was maintained at 150 °C for 20 min for all the devices. As shown in Fig. 8, the EQE of the device annealed at 120 °C is higher than the ones annealed at 110, 130, and 140 °C. Table 4 shows the power conversion efficiency, fill factor, open circuit voltage, and short circuit current density of the P3OT–PCBM interdiffused devices under monochromatic (470 nm) as well as AM1.5 illumination. The decrease in efficiency for annealing at temperatures >120 °C is presumably due to the onset of degradation.

Table 4
Monochromatic and AM1.5 power conversion efficiency, fill factor, open circuit voltage, and short circuit current density for interdiffusion with varied annealing temperatures and interdiffusion done at 150 °C for 20 min.

Annealing temperature (10 min) (°C)	Efficiency 470 nm (%)	Efficiency AM1.5G (%)	FF 470 nm	FF AM1.5G	V_{oc} 470 nm (V)	V_{oc} AM1.5G (V)	J_{sc} 470 nm (mA/cm^2)	J_{sc} AM1.5G (mA/cm^2)
110	0.75	0.3	0.4	0.36	0.395	0.515	−0.185	−1.6
120	2.0	1.0	0.5	0.44	0.385	0.525	−0.395	−4.1
130	0.9	0.3	0.39	0.32	0.365	0.515	−0.228	−1.73
140	0.7	0.3	0.41	0.33	0.375	0.555	−0.171	−1.49

4. Summary

We have reported a systematic study of the photovoltaic performance of concentration gradients of P3OT and PCBM created by thermally-induced interdiffusion of a bilayer formed through two sequential spin-casting steps. An AM1.5G power conversion efficiency of 1.0% was obtained for devices in which a 70 nm P3OT film is annealed at 120 °C followed by spin-casting of 40–50 nm thick PCBM from pyridine and interdiffusion of the two films at 150 °C for 20 min. The increased crystallinity from annealing of the P3OT film was found not to hinder the interdiffusion process and led to increased efficiency. The short circuit current density, open circuit voltage, fill factor, and power conversion efficiency were studied as a function of the thicknesses of the P3OT and PCBM layers as well as time and temperature of the interdiffusion step. Auger spectroscopy concentration depth profile studies confirmed that the maximum efficiency is obtained when the concentration gradient of the two materials spans the entire film.

Acknowledgements

This work was supported by the National Science Foundation through Grant ECS-0524625. We gratefully acknowledge the discussion on the choices of solvent with Dr. Martin Drees at Luna nanoWorks, Danville, VA.

References

[1] S. Gunes, H. Neugebauer, N.S. Sariciftci, Conjugated polymer-based organic solar cells, Chem. Rev. 107 (2007) 1324–1338.
[2] B.C. Thompson, J.M.J. Frechet, Polymer–fullerene composite solar cells, Angew. Chem. Int. Ed. 47 (2008) 58–77.
[3] W. Ma, C. Yang, X. Gong, K. Lee, A.J. Heeger, Thermally stable, efficient polymer solar cells with nanoscale control of the interpenetrating network morphology, Adv. Funct. Mater. 15 (2005) 1617–1622.
[4] G. Dennler, C. Lungenschmied, H. Neugebauer, N.S. Sariciftci, Flexible, conjugated polymer–fullerene-based bulk heterojunction solar cells: basics, encapsulation, and integration, J. Mater. Res. 20 (2005) 3224–3233.
[5] F.C. Krebs, H. Spanggard, T. Kjaer, M. Biancardo, J. Alstrup, Mater. Sci. Eng. B 138 (2007) 106–111.
[6] E. Bundgaard, F.C. Krebs, Low bandgap polymers for organic photovoltaics, Sol. Energy Mater. Sol. Cells 91 (2007) 954–985.
[7] M. Jorgensen, K. Norman, F.C. Krebs, Stability/degradation of polymer solar cells, Sol. Energy Mater. Sol. Cells 92 (2008) 686–714.
[8] D. Vacar, E.S. Maniloff, D.W. McBranch, A.J. Heeger, Charge-transfer range for photoexcitations in conjugated polymer/fullerene bilayers and blends, Phys. Rev. B 56 (1997) 4573–4577.
[9] J.J.M. Halls, K. Pichler, R.H. Friend, S.C. Moratti, A.B. Holmes, Exciton diffusion and dissociation in a poly(p-phenylenevinylene)/C-60 heterojunction photovoltaic cell, Appl. Phys. Lett. 68 (22) (1996) 3120–3122.
[10] A. Haugeneder, M. Neges, C. Kallinger, W. Spirkl, U. Lemmer, J. Feldmann, U. Scherf, E. Harth, A. Gügel, K. Müllen, Exciton diffusion and dissociation in conjugated polymer/fullerene blends and heterostructures, Phys. Rev. B 59 (1999) 15346–15351.
[11] M. Drees, K. Premaratne, W. Graupner, J.R. Heflin, R.M. Davis, D. Marciu, M. Miller, Creation of a gradient polymer–fullerene interface in photovoltaic devices by thermally controlled interdiffusion, Appl. Phys. Lett. 81 (2002) 4607–4609.
[12] M. Drees, R.M. Davis, J.R. Heflin, Thickness dependence, in situ measurements, and morphology of thermally controlled interdiffusion in polymer-C60 photovoltaic devices, Phys. Rev. B 69 (2004) 165320.1–165320.6.
[13] M. Drees, R.M. Davis, J.R. Heflin, Improved morphology of polymer–fullerene photovoltaic devices with thermally induced concentration gradients, J. Appl. Phys. 97 (2005) 036103–036103-3.
[14] M. Granstrom, K. Petritsch, A.C. Arias, A. Lux, M.R. Andersson, R.H. Friend, Laminated fabrication of polymeric photovoltaic diodes, Nature 395 (1998) 257–260.
[15] L. Chen, D. Godovsky, O. Inganas, J.C. Hummelen, R.A.J. Janssens, M. Svensson, M.R. Andersson, Polymer photovoltaic devices from stratified multilayers of donor–acceptor blends, Adv. Mater. 12 (2000) 1367–1370.
[16] J. Xue, B.P. Rand, S. Uchida, S.R. Forrest, A hybrid planar-mixed molecular heterojunction photovoltaic cell, Adv. Mater. 17 (2005) 66–71.
[17] M. Al-Ibrahim, H.-K. Roth, M. Schroedner, A. Konkin, U. Zhokhavets, G. Gobsch, P. Scharff, S. Sensfuss, The influence of the optoelectronic properties of poly (3-alkylthiophenes) on the device parameters in flexible polymer solar cells, Org. Electron. 6 (2005) 65–77.
[18] D. Gebeyehu, C.J. Brabec, F. Padinger, T. Fromherz, J.C. Hummelen, D. Badt, H. Schindler, N.S. Sariciftci, The interplay of efficiency and morphology in photovoltaic devices based on interpenetrating networks of conjugated polymers with fullerenes, Synth. Met. 118 (2001) 1–9.
[19] D. Chirvase, J. Parisi, J.C. Hummelen, V. Dyakonov, Influence of nanomorphology on the photovoltaic action of polymer–fullerene composites, Nanotechnology 15 (2004) 1317–1323.